Discriminating Crystal Binding from the Atomic Trapping of a Core Electron at Energy Levels Shifted by Surface Relaxation or Nanosolid Formation

Chang Q. Sun,* B. K. Tay, Y. Q. Fu, S. Li, and T. P. Chen

School of Electrical and Electronic Engineering, Nanyang Technological University, Singapore 639798

H. L. Bai and E. Y. Jiang

Institute of Advanced Materials Physics and Faculty of Science, Tianjin University, Tianjin 300072, P. R. China

Received: September 18, 2002; In Final Form: November 4, 2002

On the basis of the atomic-coordination−atomic-radius correlation (Feibelman, P. J. *Phys. Rev. B* **1996**, *53*, 13740. Goldschmidt, V. M. *Ber. Dtsch. Chem. Ges.* **1927**, *60*, 1270.) and its perturbation of the Hamiltonian of an extended solid, we have developed an effective yet straightforward method to determine the core-level energies of an isolated atom and the crystal-binding intensities of the core electrons at energy levels shifted by bulk formation, surface relaxation, or nanosolid formation. The developed method not only allows the predicted size dependence of core-level shift to match observations but also enables conventional X-ray photoelectron spectroscopy (XPS) to provide comprehensive information about the behavior of electrons in the deeper shells of an isolated atom and the influence of crystal formation.

Being able to discriminate crystal binding from atomic trapping of a core electron in a solid is of great scientific importance and seems to go beyond currently available experimental techniques and theoretical approaches. With laser cooling technology, one can measure the energy separation between different energy levels of the slowly moving gaseous atoms trapped by the laser beams but hardly the individual core-level energy of the isolated atom.[1] What one can measure using X-ray photoelectron spectroscopy (XPS) are the broad peaks of the core levels resulting from contributions of atomic trapping and crystal binding and the effects of crystal orientation, surface relaxation, or nanosolid formation. Besides the well-known chemical shift caused by the core−hole "screen weakening" due to charge transportation, relaxed surface atomic layers split the core level of a specimen into components, as illustrated in Figure 1. XPS measurements[2−6] reveal that the peak position of the high-energy component does not change with experimental conditions whereas the intensity of the high-energy component often increases either upon reducing the incident beam energy or upon increasing the angle between the incident beam and the surface normal in measurements. Obviously, such an intensity change arises from the varied penetration depth of the incident irradiation beams and hence confirms the surface-induced positive shift. When a solid reduces its size down to the nanometer scale, the entire core-level features move simultaneously toward high binding energy, and the amount of shift is size-dependent. For instance, both the main core-level peaks and the oxide satellites of Cu $2p_{3/2}$ (−932.1, −940.1 eV),[7] Sn 3d (−484.4, −486.7 eV), Sn 4d (−26, −31 eV), Ta $4f_{5/2}$ (−23.4, −26.8 eV), and Ta $4f_{7/2}$ (−31.6, −36.5 eV)[8] nanosolids are observed to shift up spontaneously upon reducing the particle dimension. The monopeaks of the S 2p and the S 2s core bands of the bulk ZnS (1.8−3.5 nm) and CdS solids (2.5−4.5 nm) split into three components each of the S 2p and S 2s core bands[9,10] upon the solid size being reduced. These components are associated with contributions, from high to low binding energy, of the outermost capping layer (0.2−0.3 nm thick), the second surface layer (0.2−0.3 nm thick), and the bulk core of the nanosolid. Interestingly, the peak position of each component shifts up slightly with particle dimension reduction, and hence the resultant peak position varies with the volume portion of the capping, the surface, and the core constituent of the nanosolid. When the particle size is reduced, the intensity of the core component decreases while that of the two surface components increases, which follows the size dependence of the surface-to-volume ratio of a nanosolid. This has led to an effective and competent technique[9,10] for particle size determination. Recently, Yang and Sacher[11] found that the Cu $2p_{3/2}$ peak shifts positively with particle size reduction, D, which follows the relation $\Delta E_C(D) = A + B/D$, where A and B are constants depending on both surface treatment and substrate type. Nitridation of the sample could raise the slope B from 2.1 (Cu/graphite) to 4.4 (Cu−N/polymer), demonstrating nicely the joint physical and chemical effects on the core-level shift of Cu. Therefore, as physical origin phenomena (without charge

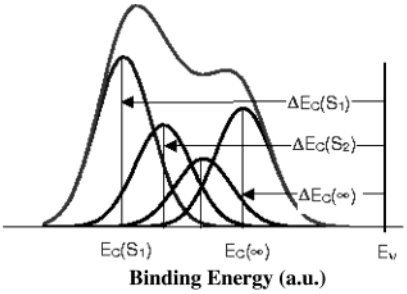

Figure 1. Illustration of the positive shift (S_1, S_2,..., B) of the core-band components and their relation to the core level of an isolated atom (E_v). $\Delta E_C(S_i) = \Delta E_C(\infty)[1 + \Delta_i]$.

* Corresponding author. E-mail: ecqsun@ntu.edu.sg. Fax: 65-6792-0415. http://www.ntu.edu.sg/home/ecqsun/.

10.1021/jp027027k CCC: $25.00
Published on Web 12/18/2002

transport being involved), surface relaxation and nanosolid formation play equivalent roles in splitting and shifting the core levels of a specimen.

Unfortunately, it seems impractical with currently available means for one to determine the energy of individual core levels of an isolated atom and to differentiate the core-level shift caused by the aforementioned origins. In this letter, we report an effective and straightforward method that allows us to gain such information with conventional XPS.

Extending the earlier conventions[12−15] of atomic-CN−atomic-radius correlation to the situation of a flat surface or a nanosolid with a curved surface, where the CN (coordination number) is reduced, a bond order−length−strength (BOLS) correlation mechanism[16,17] has been developed for the anomalous behavior of the surface and the nanosolid. The BOLS premise tells us briefly that[17] the CN imperfection of an atom at a surface causes the remaining bonds of the lower-coordinated surface atom to contract spontaneously, with an associated increase in the magnitude of the binding energy (ϵ). The CN(z_i) dependence of the reduced bond length, $c_i(z_i)$, and the bond-energy rise follow the relations

$$\begin{cases} c_i = d_i/d_0 = 2/[1 + \exp((12 - z_i)/8z_i)] \\ \epsilon_i = c_i^{-m}\epsilon_0 \end{cases} \quad (1)$$

where m is an adjustable parameter used to describe the bond-energy−bond-length correlation for different bond natures involved in the solids. For compounds and alloys, m is around 4; for elemental solids, m is around unity.[17] To cover both of the possible spontaneous relaxations, we may let $c_i < 1$, $m > 0$ for bond contraction and $c_i > 1$, $m < 0$ for bond expansion. i ranges from 1 to 3 from the outermost atomic layer to the center of the solid, respectively, as no CN imperfection is expected when $i > 3$. d_0 and ϵ_0 are the corresponding bulk values of the bond length and the single-bond energy. Exercises revealed that $z_1 = 4$, $z_2 = 6$, and $z_3 = 8$ worked sufficient well for a flat or a slightly curved surface. For a spherical dot, z_1 follows the relation $4(1 - 0.75/K)$, and $K = R/d$ is the number of atoms lined up along the radius of the spherical solid.

The bond-energy rise contributes not only to the cohesive energy (E_{coh}, being the product of the single-bond energy and the effective CN) of the surface atom but also to the energy density in the relaxed region. The modified E_{coh} dominates thermodynamic properties such as the phase transition or liquidation of the solid. The rise in the energy density provides a positive perturbation to the overall potential of the Hamiltonian of an extended solid:

$$V = V_{atom}(r) + V_{cry}(r + R_C)[1 + \Delta] \quad (2)$$

The intra-atomic trapping potential, $V_{atom}(r)$, defines the core-level position of an isolated atom. The crystal potential of an extended solid, $V_{cry}(r + R_C)$, sums the interatomic bonding to electrons in the particular site r over the entire solid, which defines the bulk shift. R_C is the lattice constant. Δ, being independent of the particular form of the interatomic potential, is the contribution from surface relaxation or nanosolid formation:

$$\Delta = \begin{cases} \Delta(S_i) = \dfrac{\Delta v(d_i)}{v(d)} = \dfrac{\epsilon_i - \epsilon_0}{\epsilon_0} = c_i^{-m} - 1 > 0 \\ \Delta(D_j) = \displaystyle\sum_{i\le 3} \gamma_{i,j}\,\Delta(S_i) + \delta \end{cases}$$

$$\gamma_{ij} = \frac{D^{\tau}_{out,i} - D^{\tau}_{in,i}}{D^{\tau}_j} \propto \frac{\tau c_i}{K_j} \quad (3)$$

$\gamma_{i,j}$ is the number or volume ratio of atoms in the ith atomic layer to that of the entire spherical solid of size $D_j = 2K_jd_0$. $D_{out,i}$ and $D_{in,i}$ correspond to the outer and inner diameter of the ith atomic layer of thickness d_i ($d_i = D_{out,i} - D_{in,i} = c_id_0$). $\tau = 1$, 2, and 3 represents the dimensionality of a spherical dot, rod, and thin plate, respectively. $\Delta(S_i)$ is the perturbation from the relaxed-surface atomic layers. $\Delta(D_j)$ is the average contribution of the entire nanosolid arising from the outermost atomic layers. The binding-energy density $v(d_i)$ is proportional to the single-bond energy, ϵ_i, as the bond number density does not change within the circumferential neighboring layers upon relaxation. δ, being the intercluster interaction, is negligibly small compared with the interatomic interaction. $\sum_{i\le 3}\gamma_i$ drops in a D_j^{-1} fashion from unity (at $K \le 3$) to infinitely small when the solid grows in dimension from the atomic to the macroscopic scale.[16]

According to band theory, the energy dispersion of a core band for an extended solid follows the relation

$$E(k) = E_v + \Delta E_C(\infty) + \Delta E_B(k, z, R_C) \quad (4)$$

where E_v is the core-level position of an isolated atom and k is a wavevector. $\Delta E_C(\infty)$ is the bulk shift of the core level, depending functionally on V_{cry} and the corresponding core−electron Bloch wave function. ΔE_B, being the width of the core band, also varies with V_{cry} and the effective CN(z) of the specific atom. Therefore, the core-level shift due to surface relaxation and nanosolid formation ($S_i \rightarrow D_j$) becomes

$$\Delta E_C(S_i) = \Delta E_C(\infty)(1 + \Delta_i) \text{ or}$$
$$E_C(S_i) - E_v = (E_C(\infty) - E_v)(1 + \Delta_i) \quad (5.1)$$

This leads to

$$\frac{E_C(S_i) - E_v}{E_C(S_{i'}) - E_v} = \frac{1 + \Delta_i}{1 + \Delta_{i'}} \qquad (i' \neq i) \quad (5.2)$$

A simple solution to eq 5.2 is

$$\begin{cases} E_v = \dfrac{(1 + \Delta_{i'})\,E_C(S_i) - (1 + \Delta_i)\,E_C(S_{i'})}{\Delta_{i'} - \Delta_i} \qquad (i \neq i') \\ \Delta E_C(\infty) = E_C(\infty) - E_v \end{cases} \quad (6)$$

Δ_i can be either $\Delta(S_i)$ for a surface or $\Delta(D_j)$ for a nanosolid (see eq 3). Equation 5.1 is the right expression for the size-and-shape-dependent core-level shift of a nanosolid if $\Delta(S_i) = \Delta(D_j)$.[16]

Not surprisingly, given an XPS profile with clearly identified $E_C(S_i)$ and $E_C(\infty)$ components of a surface or a set XPS data collected from a certain type of nanosolid of different sizes, one can easily calculate the atomic E_v and the $\Delta E_C(\infty)$ with eq 6. If n (>2) components are given, E_v and $\Delta E_C(\infty)$ should take the mean value of $C_n^2 = n!/[(n - 2)!2!]$ possible combinations with a standard error of σ because neither E_v nor $\Delta E_C(\infty)$ change with size variations or surface relaxation. This approach involves no assumptions or freely adjustable parameters. The adjustability of m reflects the variation of the bond nature. The accuracy of the determination is subject strictly to the XPS data calibration and the bond length that may not always exactly follow eq 1. Nevertheless, with this approach, we would be able to elucidate

TABLE 1: Calculated Atomic E_v, Bulk Shift $\Delta E_C(\infty)$, and the Standard Deviation σ for Different Surfaces and Nanosolids Based on the Available XPS Database[a]

	XPS measurement			calculated			calculated on the basis of the refined $E_C(S_2)$			
surface	$E_C(S_1)$	$E_C(S_2)$	$E_C(\infty)$	E_v	$\Delta E_C(\infty)$	σ	$E_C(S_2)$-refined	E_v	$\Delta E_C(\infty)$	σ (<0.1%)
poly C 1s [2]	284.42		284.30	283.46	0.84					
Ru(0001) $3d_{1/2}$ [24]	280.21	280.10	279.73	276.35	3.38	1.27(37%)	279.955	276.344	3.3856	0.003
W(110) $4f_{7/2}$ [25]	31.50	31.36	31.19	29.00	2.18	0.22(10%)	31.335	29.006	2.1835	0.003
Nb(100) $3d_{5/2}$ [4]	202.80	202.44	202.31	198.85	3.45	0.86(25%)	202.54	198.856	3.4544	0.002
Be(10$\bar{1}$0) 1s [26]	111.85	111.3	111.1	105.81	5.29	1.31(25%)	111.475	105.464	5.6355	0.002
nanosolid										
CdS−S $2p_{3/2}$ [9]	163.9	162.7	161.7	158.56	3.14	0.002				
ZnS−S 2p [10]	164.0	162.4	161.4	157.69	3.71	0.002				
CdS−S 2s [9]	226.0	224.7	223.8	220.66	3.14	0.001				
ZnS−S 2s [10]	229.0	227.3	226.3	222.32	3.92	0.001				
CuO−Cu $2p_{3/2}$ [7]	936.0/934.9 ($^4/_6$ nm)	932.9 (25 nm)	932.1 (bulk)	919.47	12.63	0.36(2.8%)	935.95(4) 934.85(6) 932.95(25)	919.58	12.52	0.30(2.4%)

[a] For elemental surfaces, $m = 1$; for compounds, $m = 4$. $z_1 = 4$, $z_2 = 6$, and $z_3 = 8$ (for nanosolids) are used in calculations with eqs 1, 3, and 6. A refinement of $E_C(S_2)$ within the XPS resolution reduces the σ to <0.1%, indicating the importance of accuracy in the XPS calibration.

the core-level positions of an isolated atom and the strength of crystal binding using the conventional XPS measurement.

There exists profound evidence for the BOLS correlation and its enormous effects on various physical properties of a nanosolid (see ref 17 and citations therein). For instance, the BOLS perturbation of the Hamiltonian expands the band gap of a nanometric semiconductor, and as a result, the dielectric is depressed, and a blue shift occurs for the photoemission and photoabsorption of nanometric semiconductors.[18] The BOLS correlation enhances the surface stress of TiCrN by about 100%.[19] The enhanced surface stress contributes to the Gibbs free energy that determines the transition behavior of the ferroelectric and pyroelectric properties of nanometric PZT oxides.[20] The BOLS-modified E_{coh} suppresses the critical temperature for the ferromagnetic phase transition and for the liquidization of nanosolids.[21]

Table 1 compares the calculated E_v, $\Delta E_C(\infty)$, and σ values for typical samples. The small σ values mean that the XPS measurement is reliable. The small σ values also prove that the BOLS correlation describes real situations adequately and that the parameters m and z_i approach their true values. Interestingly, a slight refinement of $E_C(S_2)$ (within the XPS resolution) reduces the σ values to less than 0.1%, indicating the criticality of XPS precision for the accuracy of determination and the sensitivity and reliability of the developed method. Among the analyzed surfaces, graphite (~0.8 eV) shows the weakest crystal binding whereas Be (~5.6 eV) exhibits the strongest. Calculation results from counting all of the capping, surfaces, and cores of the ZnS and CdS nanosolids show that the crystal binding of ZnS to the S 2p core level is stronger than that of CdS. The core-level energy of an isolated atom, E_v, should not change under any circumstances. However, the crystal binding to the same levels of an atom may be offset when the atom forms compounds with different elemental atoms. Surface charging also affects the measurement. Therefore, the measured S 2s and S 2p peaks of CdS should shift up or down consistently against the same peaks of ZnS. Compared with the measured S 2s and S 2p peaks from CdS, the S 2p peak from ZnS goes down slightly whereas the S 2s peak floats up with respect to those of CdS. This may cause the E_v values for the S 2s and S 2p levels in the two samples to vary slightly.

The modeling predictions agree with the observed $\Delta E_C(D)/\Delta E_C(\infty) \propto D^{-1}$ trends of O−Sn, O−Ta, CdS, and ZnS as well as Cu/graphite and (Cu−N)/polymer nanocompounds in addition to those for CuO nanosolids (with the resultant physical and chemical shift of ~21 eV).[17] The core-level shifts of all of the aforementioned nanosolids follow the D^{-1} trend when the particles are larger than the critical size (three atomic layers) below which the surface-to-volume ratio approaches unity rather than infinity.

The original 12.5-eV bulk shift of Cu $2p_{3/2}$ is shifted ~8 eV further by chemical reaction[7] and ~4 eV further by a physical size reduction to 4 nm. This agrees with the results observed from Ru(0001) and Rh(100) surfaces with and without oxidation. Upon oxidation, the two distinct Ru $3d_{5/2}$ core-level components of a clean Ru(0001) surface shift up further by up to 1.0 eV.[22] The 0.65-eV separated components of the clean Rh(100) surface shift 0.40 eV upward with oxygen addition.[23] Therefore, the chemical and physical effects enhance each other on the core-level shift, and they can be differentiated separately with the present modeling approach, providing knowledge about the relative crystal-binding intensities due to bond formation and bond relaxation.

In summary, the BOLS correlation has enabled us to attribute the core-level physical shift induced by surface relaxation and nanosolid formation to the same origin of surface CN imperfection and its positive perturbation of the Hamiltonian. Most strikingly, given an XPS profile with surface contributions or a set of XPS data from a nanosolid of different sizes, the described approach allows one to differentiate separately not only the core-level positions of an isolated atom but also its shift due to bulk formation, chemical reaction, and surface relaxation or nanosolid formation. Both the high reliability of σ in calculations and the consistency in the size-induced trend of the core-level shift provide evidence of the adequacy of the BOLS correlation in describing the real situation and the true values of CN imperfection and its effect on the core-level shift. Additionally, this approach expands the capacity of the conventional XPS technique in revealing detailed information about the behavior of electrons in deeper bands of a solid.

References and Notes

(1) Phillips, W. D. *Rev. Mod. Phys.* **1998**, *70*, 721.

(2) Balasubramanian, T.; Andersen, J. N.; Walldén, L. *Phys. Rev. B* **2001**, *64*, 205420.

(3) Aldén, M.; Skriver, H. L.; Johansson, B. *Phys. Rev. Lett.* **1993**, *71*, 2449.

(4) Fang, B. S.; Lo, W. S.; Chien, T. S.; Leung T. C.; Lue, C. Y.; Chan C. T.; Ho, K. M. *Phys. Rev. B* **1994**, *50*, 11093.

(5) Navas, E.; Starke, K.; Laubschat, C.; Weschke, E.; Kaindl, D. *Phys. Rev. B* **1993**, *48*, 14753.

(6) Bartynski, R. A.; Heskett, D.; Garrison, K.; Watson, G.; Zehner, D. M.; Mei, W. N.; Tong, S. Y.; Pan, X. *J. Vac. Sci. Technol., A* **1989**, *7*, 1931.

(7) Borgohain, K.; Singh, J. B.; Rao, M. V. R.; Shripathi, T.; Mahamuni, S. *Phys. Rev. B* **2000**, *61*, 11093.

(8) Schmeisser, D.; Böhme, O.; Yfantis, A.; Heller, T.; Batchelor, D. R.; Lundstrom, I.; Spetz, A. L. *Phys. Rev. Lett.* **1999**, *83*, 380.

(9) Nanda, J.; Kuruvilla, B. A.; Sarma, D. D. *Phys. Rev. B* **1999**, *59*, 7473.

(10) Nanda J.; Sarma, D. D. *J. Appl. Phys.* **2001**, *90*, 2504.

(11) Yang D. Q.; Sacher, E. *Appl. Surf. Sci.* **2002**, *195*, 187.

(12) Goldschmidt, V. M. *Ber. Dtsch. Chem. Ges.* **1927**, *60*, 1270.

(13) Pauling, L. *J. Am. Chem. Soc.* **1947**, *69*, 542.

(14) Feibelman, P. J. *Phys. Rev. B* **1996**, *53*, 13740.

(15) Sun, C. Q.; Bai, C. L. *J. Phys. Chem. Solids* **1997**, *58*, 903.

(16) Sun, C. Q.; Chen, T. P.; Tay, B. K.; Li, S.; Huang, H.; Zhang, Y. B.; Pan, L. K.; Lau, S. P.; Sun, X. W. *J. Phys. D: Appl. Phys.* **2001**, *34*, 3470.

(17) Sun, C. Q.; Tay, B. K.; Zeng, X.; Li, S.; Chen, T. P.; Zhou, J.; Bai, H.; Jiang, E. Y. *J. Phys.: Condens. Matter* **2002**, *14*, 7781.

(18) Sun, C. Q.; Li, S.; Tay, B. K.; Chen T. P. *Acta Mater.* **2002**, *50*, 4687.

(19) Sun, C. Q.; Tay, B. K.; Lau, S. P.; Sun, X. W.; Zeng, X. T.; Bai, H.; Liu, H.; Liu, Z. H.; Jiang, E. Y. *J. Appl. Phys.* **2001**, *90*, 2615.

(20) Huang, H.; Sun, C. Q.; Zhang, T. S.; Hing, P. *Phys. Rev. B* **2001**, *63*, 184112.

(21) Sun, C. Q.; Wang, Y.; Tay, B. K.; Li, S.; Huang, H.; Zhang, Y. B. *J. Phys. Chem. B* **2002**, *106*, 10701.

(22) Karlsson, C. K.; Landemark, E.; Chao, Y. C.; Uhrberg, R. I. G. *Phys. Rev. B* **1994**, *50*, 5767.

(23) Zacchigna, M.; Astaldi, C.; Prince, K. C.; Sastry, M.; Comicioli, C.; Rosei, R.; Quaresima, C.; Ottaviani, C.; Crotti, C.; Antonini, A.; Matteucci, M.; Perfetti, P. *Surf. Sci.* **1996**, *347*, 53.

(24) Lizzit, S.; Baraldi, A.; Groso, A.; Reuter, K.; Ganduglia-Pirovano, M. V.; Stampfl, C.; Scheffler, M.; Stichler, M.; Keller, C.; Wurth, W.; Menzel, D. *Phys. Rev. B* **2001**, *63*, 205419.

(25) Riffe, D. M.; Kim, B. J.; Erskine, L.; Shinn, N. D. *Phys. Rev. B* **1994**, *50*, 14481.

(26) Lizzit, S.; Pohl, K.; Baraldi, A.; Comelli, G.; Fritzsche, V.; Plummer, E. W.; Stumpf, R.; Hofmann, Ph. *Phys. Rev. Lett.* **1998**, *81*, 3271.